Proceedings of the ASME 2019 Manufacturing Science and Engineering Conference
MSEC2019
June 10-14, 2019, Erie, PA, USA

MSEC2019-2906

AN EXPERIMENTAL STUDY ON DIRECT CURRENT DIELESS DRAWING OF 4130 STEEL TUBES

Chetan P Nikhare
Penn State Erie – The Behrend College
Erie, PA, USA
cpn10@psu.edu

Paul McMahon
Kennedy Catholic Family of Schools
Hermitage, PA, USA
pmcmahon@kennedycatholicschools.org

Faisal Aqlan
Penn State Erie – The Behrend College
Erie, PA, USA
fua11@psu.edu

ABSTRACT

Forming of tubes in various shapes has been a major interest in vehicle, instrumentation, decoration and precision industries. Due to a variety of shapes that can be achieved by tube forming, this manufacturing process has taken a major part in research and application. In this manufacturing process, a tube with a certain diameter and thickness can be considered to shape the part. The shaping or forming can be achieved by end forming, expanding the section, bending the section, buckling the tube, and/or reducing the section. Traditionally, to form these sections the rigid tool, flexible tool or fluid pressure would be needed to shape the tube. However, tools like mandrel or plug and their sizes limit the size of the tube to be formed. In this paper, tubes are formed by stretching them while simultaneously passing the direct current through. This process has been explored earlier by heating the tube using induction heating or rotary laser heating method. However, as no dies or tools are used to form these tubes, the process is considered dieless tube drawing which involves heating the tubes and drawing them into a reduced section. This study considers two different thicknesses but the same outer diameter tubes. The drawing force, shape, and microstructure are investigated. Based on the stress-strain curve, the yield to fracture and tensile to fracture strains are determined and discussed.

INTRODUCTION

Formed tubes are used for a wide variety of applications. They are the integral parts of modern machines. The common applications are in fluid transport, load-bearing structural components, and construction. The most common uses of these hollow components include: (1) to transport fluid medium in oil and gas industry through bigger diameter tubes running under the ground, (b) to transfer oil through medium diameter tubes, and (c) passing the refrigerant for heat transfer in refrigeration through small diameter tubes or injecting the fluid medicine in human body through microtubes. In any of these cases, the tube needs to go through the forming process to meet the desired shape in the service.

Tube forming can be performed by expansion, reduction, and bending the cross-section using a solid tool, flexible tool, or internal fluid pressure. As the study related to the tube end forming by reducing the tube geometry, it comes under the category of tube end forming. This tube end forming category includes inversion, expansion, reduction [1], beading [2], nosing [2, 3], and flaring in single or multiple forming operations [4]. Out of these, flaring is the far most used process to change the tube end geometry by expanding or shaping it to a variety of shapes. In this process, the solid tool is used of a particular desired shape which then displaces from one end of the tube while another end is fixed, resulting in the expansion of the tube. To delay the failure a more generous tool followed by the sharp shape tool can be used to achieve the final shape [5]. Other studies focused on the material and process parameter influence on the tube-flaring ratio, strain path, forming limits [6-15]

Forming of metal involves cold and hot temperatures. Cold drawing increases the strength of the metal but reduces the ductileness. This occurs because dislocations in the bonds of the metal atoms form when a metal is stressed. During cold forming,

the dislocations pile up and increase the strength, and less ductility remains in the metal. The other approach to follow is hot or warm forming. Hot forming causes dislocations but the additional heat allows the dislocations to annhilate and easy path for movement which shows the reduction of stresses and increase in ductility. In this study electric current was used to pass through the tube while applying to force to stretch the tube. No literature was found using the electric current on tubes. A similar approach was performed earlier but using the induction heating on the microtube [16].

Previous studies on electrically assisted manufacturing [EAM] provides significant data, which can be learned to implement in the processes. It was noted that the mechanical properties of the metals could be influenced by passing the electric current. The current density is important to generate sufficient heat to obtain a mechanical behavior [17-22]. The material recrystallization and grain size were studied with continuous direct current [23-24]. Some work reported that the electric effect was greater than what could have been explained only with Joule heating [25-26]. Good amount of work can be found passing the electric current; however, none is on tube forming. Thus, in this study, the electric current was passed through the tube while mechanically pulling the tube to reduce the cross-section. Various current values pull rates and pulsing of current was considered. The material behavior during these tests, plastic deformation, and convergence of reduction area were discussed and analyzed.

MATERIAL

The material used in this experiment is 4130 steel rod with an outer diameter of 6.35 mm and two different thicknesses of 1.651 mm and 0.889 mm.

METHODOLOGY

Figure 1 shows a schematic of the direct current dieless drawing set up on a Tinius Olsen 60 kip 4-screw electrically driven universal test machine. Tinius Olsen Test Navigator, Version 7.02.10 was used to gather the force and displacement data. The arc welder used was a Lincoln Electric Idealarc R3S 600 with an input of 460 VAC and an output of 600A at 44V Constant Voltage at 100% Duty Cycle. The constant voltage used for the experiment was set at 18 V and the time elapse set at 5 minutes. Different currents of 150 A, 250 A, and 350 A, were produced by changing the length of metal bands and measured with an Omega HHM592D clamp-on ammeter. The metal bands were cooled by an industrial fan at its highest setting. The tube was fixed between two jaws. The upper jaw was attached to the crosshead while the lower jaw was attached to the movable platen. The lower jaw was set to displaced with two different rates. Three test categories were tested: 1) four different current densities for both tubes 0 A/mm^2 (i.e, no current passed or Baseline), 6.8, 10.5, and 13.7 A/mm^2, 2) two different rates 5 mm/min and 50 mm/min with current density of 10.5 A/mm^2, and 3) two pulsing condition with a current density of 10.5 A/mm^2.

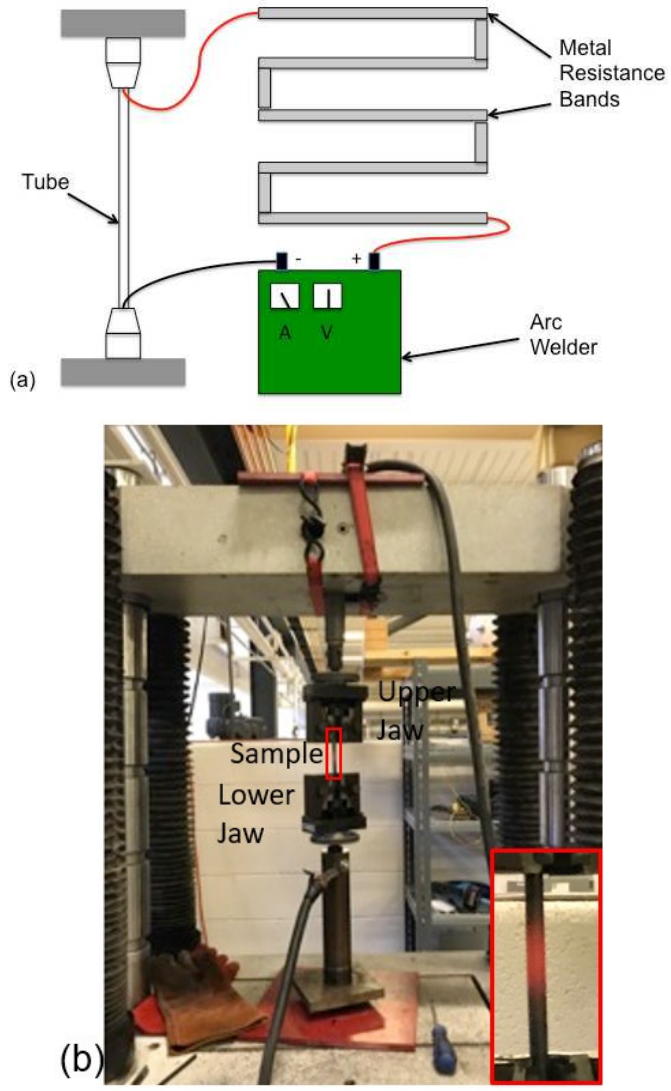

FIGURE 1. Tube forming (a) schematic illustration of dieless drawing apparatus and (b) experimental ste-up of dieless drawing apparatus.

RESULTS AND DISCUSSION

Current density

Figure 2 shows the separated half sample of tubes with necking. The draw rate was held constant at 5 mm/min. It can be seen that the fractured sample of 0 and 6.81 A/mm^2 shows the cup and cone fracture. The 10.5 A/mm^2 sample shows the highest visible necking and 13.7 A/mm^2 shows premature failure due to high resistance heating. Similar behavior has been observed with thin tubes (Figure 3). However, with the same heat generation, the thinner tube will have more heat dissipation due to higher surface area and thus the sample with 10.5 A/mm^2 does not have much different than 6.81 A/mm^2. The sample with 13.7 A/mm^2 shows a similar fracture as shown in the thick tube. It seems that a current density of higher than 10.5 and lower than 13.7 A/mm^2 would have given the better necking region.

FIGURE 2. Fractured specimen of thick tube samples with current density of 0, 6.8, 10.5 and 13.7 A/mm^2 (left to right)

FIGURE 3. Fractured specimen of thin tube samples with current density of 0, 6.8, 10.5 and 13.7 A/mm^2 (left to right)

Figure 4 shows the stress-strain curve for both the thick and thin specimens at different current densities. As these tubes had different thicknesses, the force-displacement curves were normalized to better represent the data. Due to the compliance of the machine initial displacement with negligible force was removed from the data. It can be seen that both tubes were holding their stress values at 0, and 6.8 A/mm^2. However, the stresses dropped for the thicker tube at higher current densities. This proves the same reasoning of having the higher surface area for the thinner tube to dissipate the heat faster, whereas the thicker tubes hold the heat and thus softens faster. Based on the stress-strain curve the yield strength, tensile strength, strain from yield strength to fracture and strain from tensile strength to fracture were determined. The yield strength values are based on the deviation of the curve from the linearity and not of 0.2% offset as that might have affected the tensile strength values. The values are listed in Tables 1 and 2.

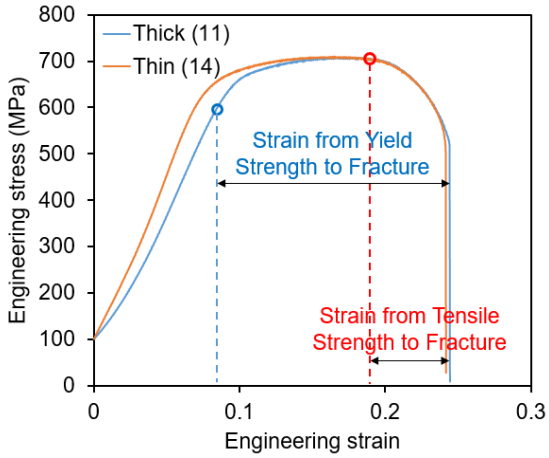

(a)

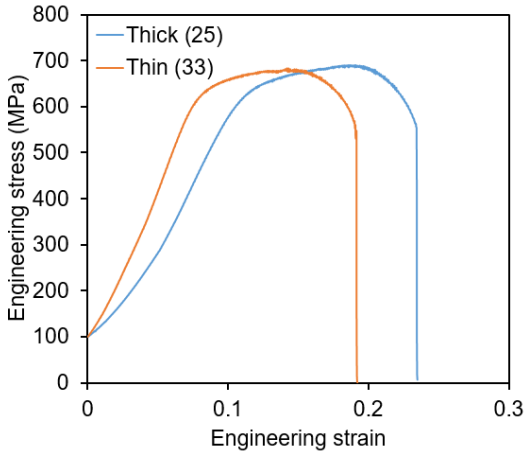

(b)

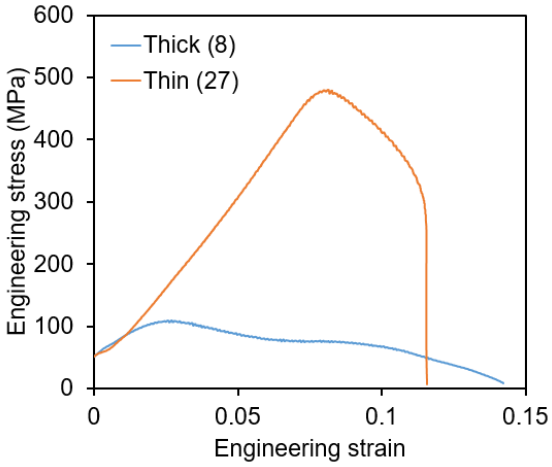

(c)

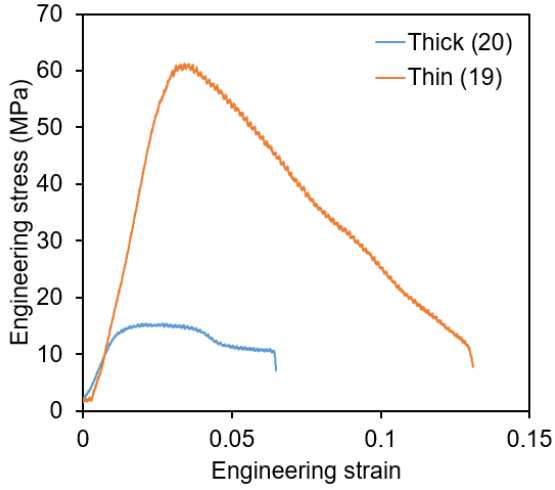

(d)

FIGURE 4. Engineering stress strain curve with varying current density (a) 0, (b) 6.8, (c) 10, and (d) 13.7 A/mm^2

TABLE 1. Thick tube properties at different current densities

Current Density (A/mm^2)	Yield Strength (MPa)	Tensile Strength (MPa)	Strain from Yield Strength to Fracture (%)	Strain from Tensile Strength to Fracture
0	594	708	16.04	7.2
6.8	560	690	13.86	4.5
10.5	97	109	12.61	11.62
13.7	11.5	15.5	5.61	3.8

TABLE 2: Thin tube properties at different current densities

Current Density (Amp/mm^2)	Yield Strength (MPa)	Tensile Strength (MPa)	Strain from Yield Strength to Fracture (%)	Strain from Tensile Strength to Fracture
0	584	710	17.43	7.7
6.8	573	683	12.22	4.9
10.5	451	480	4.33	3.44
13.7	52	61	10.67	9.68

A sudden change in the values for yield strength and tensile strength were observed for a current density of 10.5 A/mm^2 for the thick tube, but that transition was 13.7 A/mm2 for the thin tube. The strain achieved after yield strength was continuously dropping with an increase in current density for the thick tube, but for the thin tube it was found increase at transition current density. The strain achieved after tensile strength was found dropping but with an increase at transition temperature for thick tube and found a similar result for the thin tube. This data provides an indication that at the transition current density a reduced section with converge tubes can be manufactured.

Figure 5 provides the images of 2D cut section in half to observe the convergence. Thick (11), (25), (8) and (20) are the samples of the thick tube with increasing current density and the same with the thin tubes. The tubes were half cut in the longitudinal direction and were hot mounted in the 31.75 mm diameter mold. The samples were then grinded and polished for measurements. With a normal camera, all mold samples photograph were captured from a constant distance. Further, the images were post-processed by keeping the aspect ratio of mold diameter contact so not to distort the images. Please note that the image with Thick (11) was without current and did not join the tube at convergence. The tube was grinded farther and thus resulted in this image. With higher current density, when the specimen fractures the spark generates at the tip which was at much higher temperature and thus a bulb like a drop appears. If the melted pieces come together, they can join as shown in image Thick (8). If that process is delayed then the specimen will have a convergence end as shown in images Thick (20) and Thin (19).

To analyze the convergence section, approximate tangent lines at the converge ends were drawn and the angle was measured as shown in Figure 6. The convergence angle for all 8 specimens is detailed in Table 3. The higher the angle the more reduction towards convergence has happened. It can be seen that very near to the transition current density the higher convergence angle was achieved.

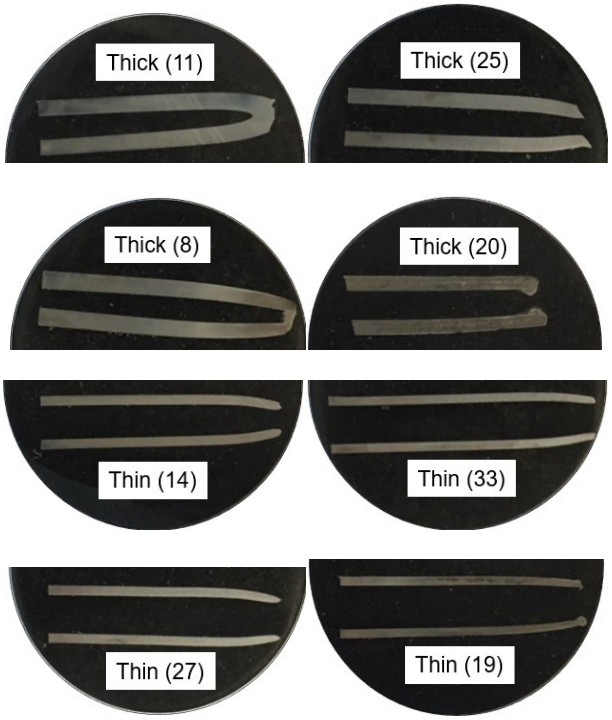

FIGURE 5. Sectional cut tubes mounted in the mold to observe the reduced section convergence

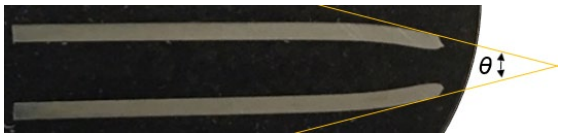

FIGURE 6. Reduced section converging angle measurement

TABLE 3. Specimen, current density and achieved reduced section convergence angle

Sample	Current Density (Amp/mm^2)	Angle (°)
Thick (11)	0	33.81
Thick (25)	6.81	26
Thick (8)	10.5	32.28
Thick (20)	13.7	4.52
Thin (14)	0	28.71
Thin (33)	6.81	25.47
Thin (27)	10.5	40
Thin (19)	13.7	26.2

After polishing all samples with 3-micron polishing compound they were etched with 3% nital solution to capture the microstructure. Figures 7-10 shows the SEM images at the crack

tip to see if there was any change in microstructure. No major differences can be seen in the microstructure until for transition temperature. At and after transition temperature the ferrite-cementite microstructure changes to the pearlite. The pearlite was developed due to the cooling of the sample was at air after it was fractured.

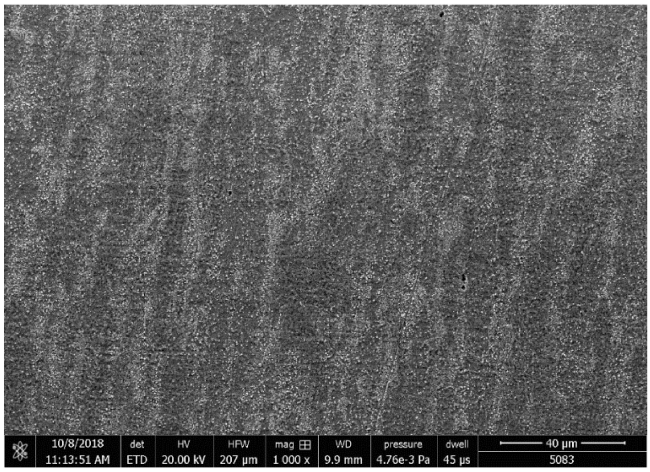

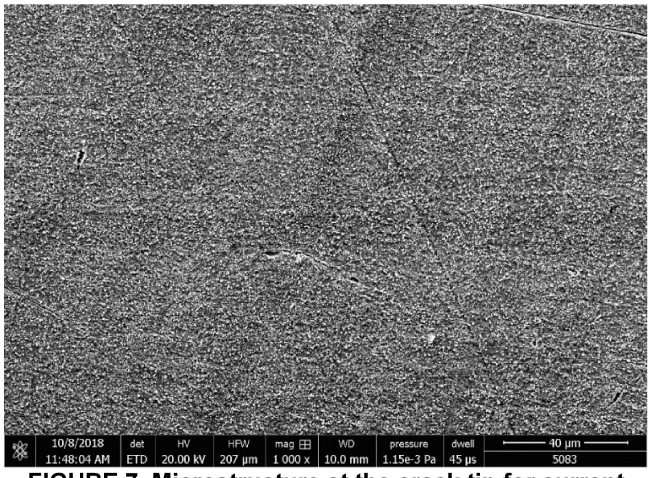

FIGURE 7. Microstructure at the crack tip for current density of 0 A/mm^2: Thick (top) and Thin (bottom)

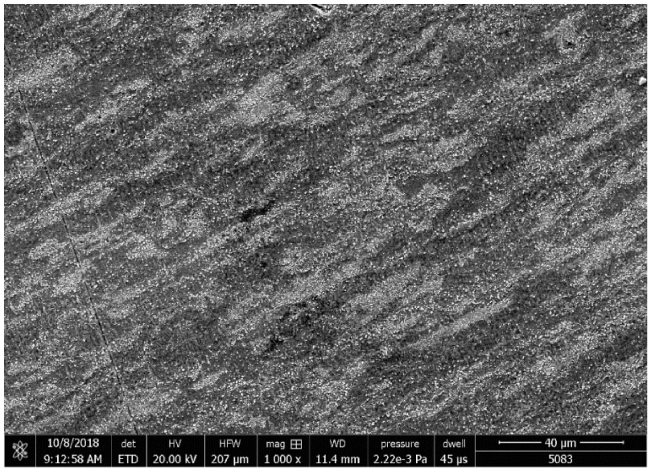

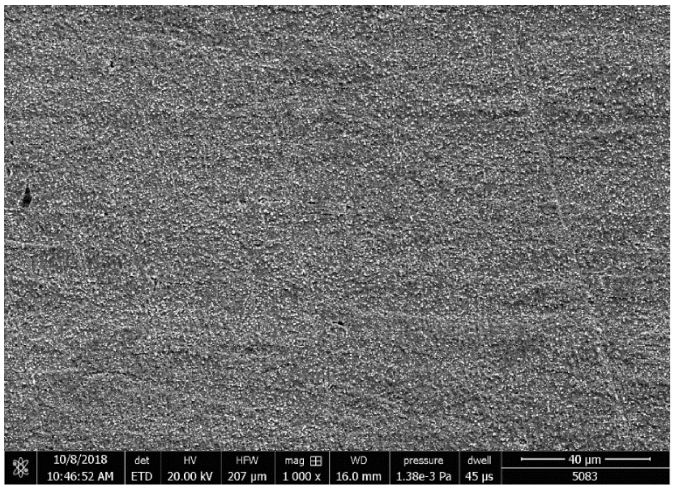

FIGURE 8. Microstructure at the crack tip for current density of 6.8 A/mm^2: Thick (top) and Thin (bottom)

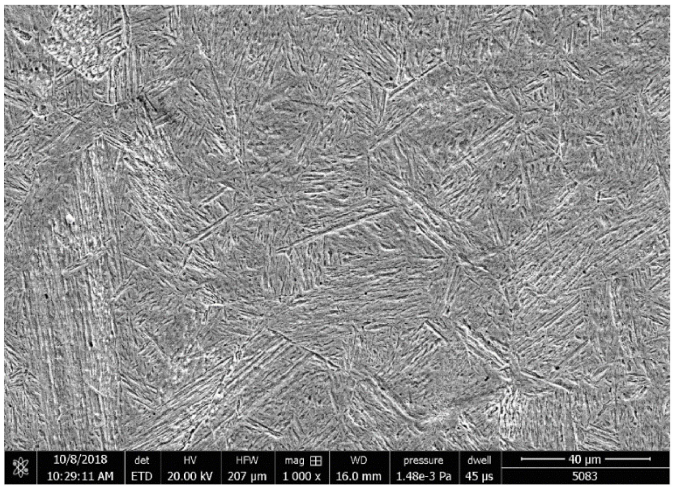

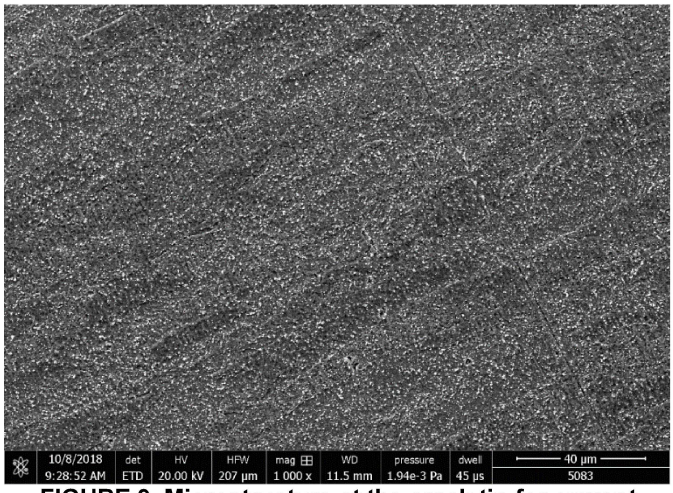

FIGURE 9. Microstructure at the crack tip for current density of 10.5 A/mm^2: Thick (top) and Thin (bottom)

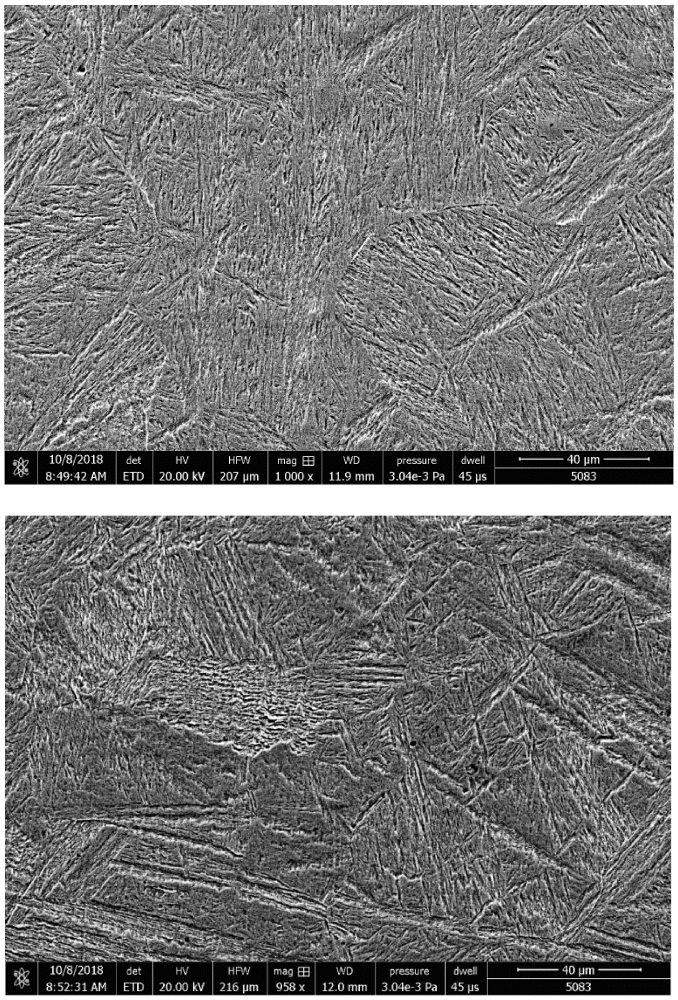

FIGURE 10. Microstructure at the crack tip for current density of 13.7 A/mm^2: Thick (top) and Thin (bottom)

FIGURE 11. Fractured specimen for thick samples with 5 and 50 mm/min

FIGURE 12. Fractured specimen for thin samples with 5 and 50 mm/min

Varying Strain Rate

The second set of experiments involved changing the rate at which the tubes were pulled i.e., 5 mm/min and 50 mm/min. The charge density was held constant at 10.5 A/mm^2. The fractured specimens are shown in Figure 11 for thick specimen (specimen 8 with 5mm/min and 6 with 50mm/min) and Figure 12 for the thin specimen (specimen 27 with 5mm/min and 30 with 50mm/min). The data shows that there is not a significant impact on the displacement between the two draw rates rather than just the softening of material at due to more time provided for testing (Thick 8) (Figure 13 and 14).

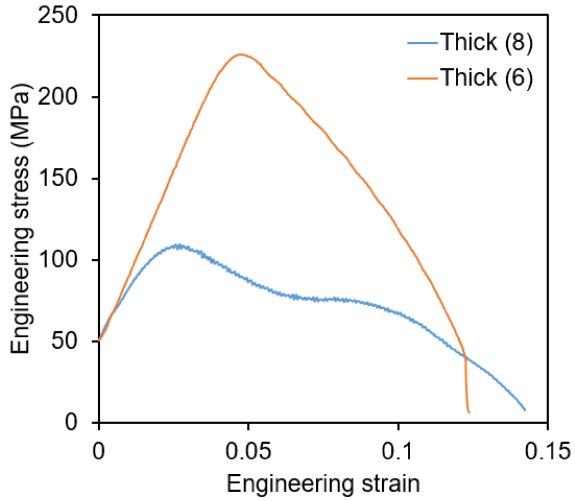

FIGURE 13. Engineering stress strain curve with varying strain rate for thick tubes

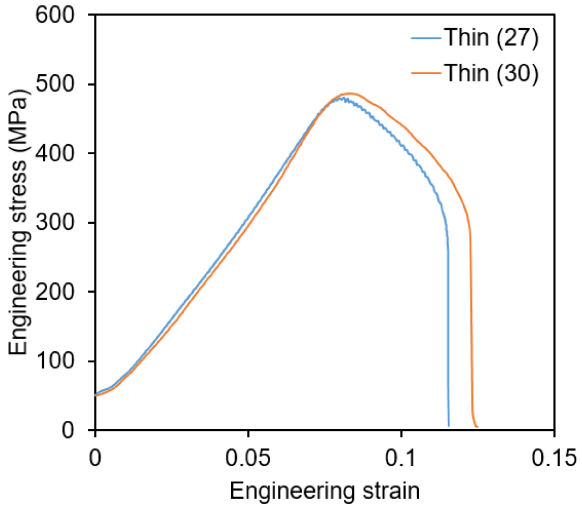

FIGURE 14. Engineering stress strain curve with varying strain rate for thin tubes

Table 4 provides the tube properties at different speeds for thick and thin tubes. It can be observed that with the higher rate the thick tubes maintain the stress level, however, no difference was observed with the thin tubes. With higher rates, the strain achieved after yield strength and tensile strength was decreased for thick tubes but it has increased for thin tubes.

TABLE 4. Thick and thin tube properties at different speed

Sample {Speed, mm/min}	Yield Strength (MPa)	Tensile Strength (MPa)	Strain from Yield Strength to Fracture (%)	Strain from Tensile Strength to Fracture
Thick (8) {5}	97	109	12.61	11.62
Thick (6) {50}	205	226	8.7	7.7
Thin (27) {5}	451	480	4.33	3.44
Thin (30) {50}	456	487	5.1	4.18

With reference to Figure 15 and Table 5, it can be seen that with an increase in rate, the thick tubes get much better convergence. Remember that 10.5 A/mm2 is the transition temperature for thick tubes. With having a transition temperature and higher pulling rate, the material maintains higher stress and thus had more time for necking. A sharp convergence appeared in sample Thick (6). However, with having pulled in non-transition temperature at the higher rate, the thin tube experiences the strain rate effect and thus provides less ductility.

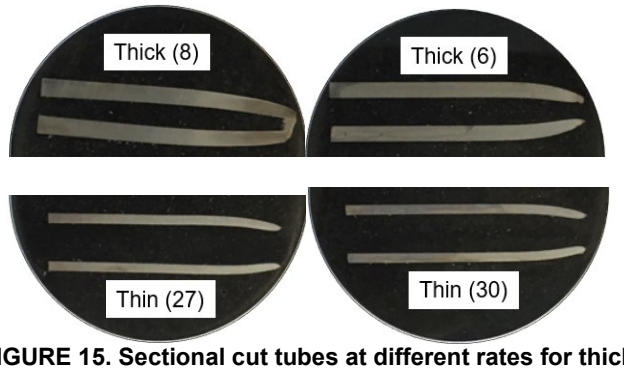

FIGURE 15. Sectional cut tubes at different rates for thick and thin tubes

TABLE 5. Specimen, speed and achieved reduced section convergence angle

Sample {Speed, mm/min}	Angle (°)
Thick (8) {5}	32.28
Thick (6) {50}	57.33
Thin (27) {5}	40
Thin (30) {50}	30.94

Varying pulsing electric current

The third set of experiments performed were based on pulsing the current. For this, a current density of 10.5 A/mm2 was used. The pulsing was set with a square waveform (Figure 16). The pulse period was kept for 60 s. Two experiments were performed, one with 30 s pulse duration and other with 15 s. The specimen pull rate was kept constant at 5 mm/min.

Figure 17 shows the fractured specimen with pulsing experiments. (37) and (46) are the thick tubes, and (40) and (42) are the thin tubes with 30 and 15 s pulse duration, respectively. All specimens failed with cup and cone fracture with short necking. This is because the specimens were intermittently cooled by pulsing. Even though the thick specimen was tested with transition current density of 10.5 A/mm2, the cooling has changed the behavior and thus all specimens maintained the stress levels as shown in Figure 18. The strain achieved after yield strength and tensile strength is decreased with more cooling time which is due to changing the material behavior from soft to hard (Table 6).

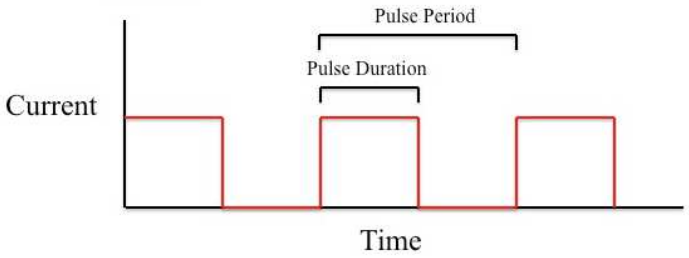

FIGURE 16. Square waveform for pulsing the current

FIGURE 17. Fractured specimen for thick (37 and 46) and thin (40 and 42) samples from pulsing experiments

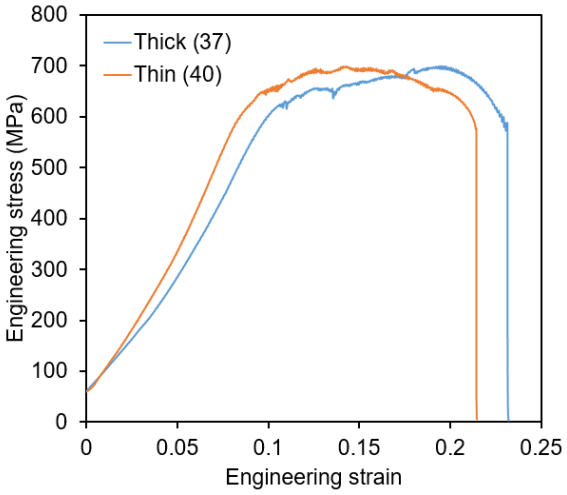

(a)

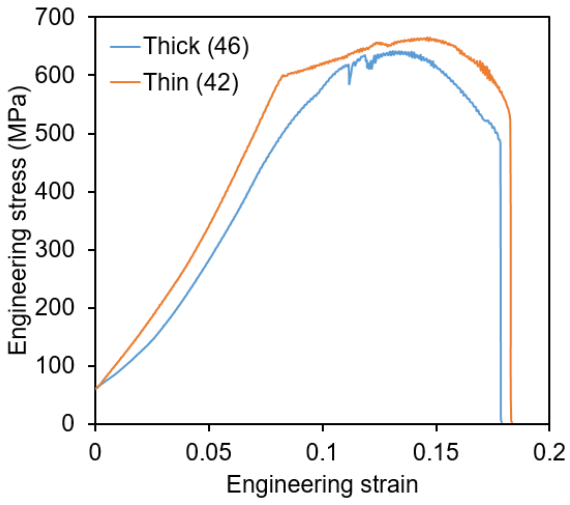

(b)

FIGURE 18. Engineering stress strain curve for pulsing current: (a) 30 s pulse duration and (b) 15 s pulse duration.

TABLE 6. Thick and thin tube properties with pulsing current (PD – Pulse Duration)

Sample	Yield Strength (MPa)	Tensile Strength (MPa)	Strain from Yield Strength to Fracture (%)	Strain from Tensile Strength to Fracture (%)
Thick (37) PD=30 s	558	699	14.01	3.8
Thick (46) PD=15 s	466	641	10.11	4.7
Thin (40) PD=30 s	580	698	13.27	7.3
Thin (42) PD=15 s	597	664	10.08	3.6

CONCLUSION

In this study, dieless drawing using direct electric current was performed on two tubes with the same outer diameter but different thicknesses to reduce the section. Three main types of experiments were performed a) with varying current densities, b) with varying pulling rates, and c) with the pulsing current. Based on the experimental results, it was observed that the tubes were having different transition current density related to the area through which the currents are passing. At this transition current density, the material stress level drastically drops. With higher surface area, the heat dissipation increases and thus higher transition current density would be needed. With increasing current density, the strain achieved after yield strength and tensile strength decreases with the only jump occurred at their transition current densities. Around transition current density, the reduced tube section with a higher convergence angle was achieved. Also, a change in microstructure was occurred at or above transition current density. With increasing pulling rate, the time provided for stretching was less and thus the softening effect was reduced and the tube performed better in thick tubes. The thinner tube had no effect with strain rate. With pulsing, the intermittent cooling of tubes occurred and thus they performed poorly. Thus a higher current density with pulsing would provide better results. To conclude the study, a dieless drawing of the tube can be achieved by passing the direct current with pulsing. This process can be utilized for precise microtubes manufacturing such as medical instruments, precision parts etc.

ACKNOWLEDGMENTS

This research is funded by the National Science Foundation NSF RET- #1711603: RET Site in Manufacturing Simulation and Automation. Any opinions, findings, or conclusions found in this paper are those of the authors and do not necessarily reflect the views of the sponsor.

The authors would like to acknowledge Penn State Behrend for providing the facilities to conduct the experiments. The authors would like to thank Glenn Craig for the fabrication of test samples.

REFERENCES

[1] Almeida, B. P. P., Alves, M. L., Rosa, P. A. R., Brito, A. G., and Martins, P. A. F., 2006, "Expansion and Reduction of Thin-Walled Tubes Using a Die: Experimental and Theoretical Investigation," Int. J. Mach. Tools Manuf., 46(12), pp. 1643–1652.

[2] Gouveia, B. P. P., Alves, M. L., Rosa, P. A. R., and Martins, P. A. F., 2006, "Compression Beading and Nosing of Thin-Walled Tubes Using a Die: Experimental and Theoretical Investigation," Int. J. Mech. Mater. Des., 3(1), pp. 7–16.

[3] Lu, Y. H., 2005, "Study of Perform and Loading Rate in the Tube Nosing Process by Spherical Die," Comput. Methods Appl. Mech. Eng., 194(25–26), pp. 2839–2858.

[4] Alves, L. M., Pardal, T. C. D., and Martins, P. A. F., 2010, "Nosing Thin- Walled Tubes Into Axisymmetric Seamless Reservoirs Using Recyclable Mandrels," J. Cleaner Prod., 18(16), pp. 1740–1749.

[7] Nikhare, C.P., Korkolis, Y.P. and Kinsey, B.L., 2015. Formability Enhancement in Titanium Tube-Flaring by Manipulating the Deformation Path. Journal of Manufacturing Science and Engineering, 137(5), p.051006.

[6] Yang, J., Luo, M., Hua, Y. and Lu, G., 2010. Energy absorption of expansion tubes using a conical–cylindrical die: experiments and numerical simulation. International Journal of Mechanical Sciences, 52(5), pp.716-725.

[7] Fischer, F.D., Rammerstorfer, F.G. and Daxner, T., 2006. Flaring—an analytical approach. International Journal of Mechanical Sciences, 48(11), pp.1246-1255.

[8] Huang, Y.M., 2009. Flaring and nosing process for composite annoy tube in circular cone tool application. The International Journal of Advanced Manufacturing Technology, 43(11), pp.1167-1176.

[9] Wang, Z.R., Kun, D. and Yi, F., 1997. The method of the principal shear stress tracing line and its application in the flaring and expanding of a thin-walled tube with a conical punch. Journal of Materials Processing Technology, 70(1-3), pp.220-227.
[10] Mirzai, M.A., Manabe, K.I. and Mabuchi, T., 2008. Deformation characteristics of microtubes in flaring test. Journal of Materials Processing Technology, 201(1), pp.214-219.
[11] Alves, M.L., Almeida, B.P.P., Rosa, P.A.R. and Martins, P.A.F., 2006. End forming of thin-walled tubes. Journal of Materials Processing Technology, 177(1), pp.183-187.
[12] Nikhare, C.P., 2012. Tube Forming Through Flaring Process With Bend-Unbend Mechanism. International Deep Drawing Research Group, Mumbai, India, pp. 172-178.
[13] Sun, Z.C. and Yang, H., 2007. Study on forming limit and feasibility of tube axial compressive process. Journal of Materials Processing Technology, 187, pp.292-295.
[14] Daxner, T., Rammerstorfer, F.G. and Fischer, F.D., 2005. Instability phenomena during the conical expansion of circular cylindrical shells. Computer Methods in Applied Mechanics and Engineering, 194(21), pp.2591-2603.
[15] Nikhare, C.P., Gone, R., 2016. Comparison of forming limits in tube and sheet forming. International Deep Drawing Research Group, Linz, Austria, pp. 50-60.
[16] Furushima, T. and Manabe, K., 2007. Experimental study on multi-pass dieless drawing process of superplastic Zn–22% Al alloy microtubes. Journal of Materials Processing Technology, 187, pp.236-240.
[17] Machlin, E. S. (1959). "Applied Voltage and the Plastic Properties of "Brittle" Rock Salt," J. Appl. Phys., 30(7), pp.1109-1110.
[18] Troitskii, O.A., (1969). "Electromechanical Effect in Metals." Pis'ma Zhurn. Experim. Teoret. Fiz., No. 10, pp. 18.
[19] Pleta, A., M. Krugh, C. Nikhare, J.T. Roth, 2013, "An Investigation of Anisotropic Behavior on 5083 Aluminum Alloy Using Electric Current." ASME Paper No. MSEC2013-1244.
[20] Lobdell, M., C. Nikhare, J.T. Roth, 2013, "Comparison of electric and thermal effects on AA5083 aluminum alloy." Proc. of IDDRG 2013, Zurich, Switzerland
[21] Pleta, A., C. Nikhare, J.T. Roth, 2013, "An electric touch for aluminum springback elimination." Proc. of IDDRG 2013, Zurich, Switzerland
[22] Andrawes, J.S., T.J. Kronenberger, J.T. Roth, and R. L. Warley (2007). "Effects of DC current on the mechanical behavior of AlMg1SiCu." Mat.and Manuf. Proc., 22 (1), pp. 91-101.
[23] Xu, Z.S., Z.H. Lai, and Y.X. Chen (1988). "Effect of Electric Current on the Recrystallization Behavior of Cold Worked Alpha-Ti." Scripta Metallurgica, 22, pp. 187-190
[24] Heigel, J.C., J.S. Andrawes, J.T. Roth, M.E. Hoque, and R.M. Ford (2005). "Viability of electrically treating 6061 T6511 aluminum for use in manufacturing processes." Trans. of the North American Manufacturing Research Institute of SME, 33, pp. 145-152.
[25] Perkins, T.A., T.J. Kronenberger, J.T. Roth (2007). "Metallic forging using electrical flow as an alternative to warm/hot working." J. of Manuf. Sci. and Engr., 129 (1), pp. 84-94
[26] Ross, C.D., D.B. Irvin, and J.T. Roth (2007). "Manufacturing aspects relating to the effects of DC current on the tensile properties of metals." J. of Engr. Mat. and Tech., 129(2), pp. 342-347.